THE JOURNAL OF PHYSICAL CHEMISTRY C
A JOURNAL OF THE AMERICAN CHEMICAL SOCIETY

pubs.acs.org/JPCC

Article

Methylidyne Adsorption on Pt(211) Probed by Reflection Absorption Infrared Spectroscopy (RAIRS)

Harmina Vejayan, Ana Gutiérrez-González, María E. Torio, H. Fabio Busnengo,* and Rainer D. Beck*

Cite This: https://doi.org/10.1021/acs.jpcc.2c07235

Read Online

ACCESS | Metrics & More | Article Recommendations | Supporting Information

ABSTRACT: Methylidyne, CH(ads), adsorbed on a Pt(211) surface and its interaction with chemisorbed hydrogen atoms was studied by reflection absorption infrared spectroscopy (RAIRS). Methylidyne was formed on Pt(211) by methane dissociation from a molecular beam followed by thermal decomposition of the methane dissociation products. CH(ads) was detected by RAIRS via its symmetric C−H stretch vibration resulting in three discrete absorption peaks in the region of 2950−2970 cm^{-1}. While the frequencies of the three C−H stretch peaks remain fixed, their relative intensities depend on the H(ads) co-coverage. This differs markedly from what was observed previously for the RAIR spectra of CH(ads) adsorbed on Pt(111) by the group of Trenary,[1] who observed a single C−H stretch peak, which showed a continuous blue shift with increasing H(ads) coverage. Based on our experimental results and density functional theory (DFT) calculations, we propose that the three discrete absorption peaks on Pt(211) are due to the adsorption of methylidyne on the steps of Pt(211) forming one-dimensional rows of adsorbates. Depending on the H(ads) coverage, the CH(ads) species on the step sites can have either zero, one, or two neighboring H(ads) atoms, leading to three different vibrational C−H stretch frequencies and a reversible shift in relative peak intensity depending on the H(ads) coverage.

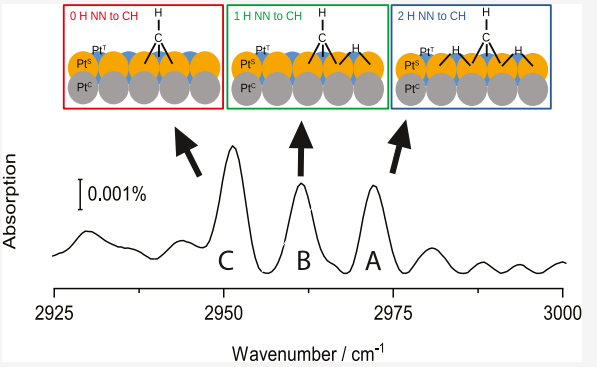

INTRODUCTION

Understanding the stability and reactivity of small hydrocarbon species CH_x (x = 1, 2, 3) adsorbed on metal surfaces is of great importance for the elucidation of the underlying mechanisms of many heterogeneous catalytic reactions such as steam reforming, water gas shift, and Fischer−Tropsch synthesis.[1−4] In this context, vicinal metal surfaces are particularly useful for surface science studies because they expose a well-characterized arrangement of terraces, steps, and kinks. Thus, they provide a good compromise between simplicity, enabling high-level theoretical modeling, and complexity by mimicking realistic active sites typically encountered in metal nanoparticles or clusters of real catalysts. Platinum is one of the transition metals commonly used as a catalyst in multiple reactions, and in spite of often being the most stable CH_x species[5,6] on Pt vicinal surfaces, methylidyne (CH) has been less studied than methyl (CH_3) and methylene (CH_2).[6−9]

Reflection absorption infrared spectroscopy (RAIRS)[10,11] is a highly sensitive and noninvasive method that provides information both on the structure and the adsorption site of chemisorbed species. Thus, combining RAIRS with supersonic molecular beam (SMB) experiments, including state-specific preparation of the reagent molecules, has enabled highly detailed measurements of the reactive sticking coefficients of methane on Pt(211) resolved by impact energy, vibrational states, and surface sites.[7] The latter experiments were performed at surface temperatures $T_s \leq 150$ K to stabilize the nascent dissociation products of methane, which were assigned to be chemisorbed methyl species on both the terrace and step sites of Pt(211).[7] Recent density functional theory (DFT) calculations[6] proposed that the methyl species adsorbed on the step sites of Pt(211) might undergo facile dehydrogenation to form chemisorbed methylene at $T_s \leq 150$ K. However, since our efforts to confirm this secondary dissociation step by experiments were unsuccessful, we will refer here to the species adsorbed on the Pt(211) step sites as methyl.

EXPERIMENTAL SECTION

In this work, we used RAIRS to investigate the thermally induced decomposition of methyl species on the steps and terraces of Pt(211) to form methylidyne (CH(ads)) with and without co-adsorbed hydrogen atoms. Experiments were performed in an ultra-high vacuum (UHV) surface science

Received: October 14, 2022
Revised: November 21, 2022

apparatus with a base pressure of 2×10^{-11} mbar coupled to a Bruker Vertex V-70 Fourier transform infrared spectrometer.[12] RAIR spectra were recorded using a liquid nitrogen-cooled InSb detector. Unless mentioned otherwise, each RAIR spectrum is the average of 2048 scans recorded at a resolution of 4 cm^{-1}. A continuous molecular beam source coupled to the UHV chamber was used to collide methane seeded in helium with controlled kinetic energy at normal incidence with the Pt(211) surface at T_s = 150 K. The Pt(211) surface was cleaned by Ar^+ sputtering at 1 kV and 2 μA for 10 min at T_s = 300 K, followed by annealing to T_s = 1100 K for 2 min. This cleaning procedure was verified by Auger electron spectroscopy (AES) to remove any C and O impurities below the 1% detection limit of the AES analysis.

To assist the assignment of the observed RAIRS peak, we performed density functional theory (DFT) calculations using a plane-wave basis set and the projected augmented wave (PAW) method[13] implemented in the VASP.[14−18] The (spin-restricted) calculations used an energy cutoff of 450 eV and the PBE generalized gradient approximation (GGA) to describe electronic exchange and correlation (XC).[19] The Pt(211) surface has been modeled within the slab-supercell approach using 9 Pt layers (perpendicular to the macroscopic surface) in a 1 × 5 supercell and a 5 × 3 × 1 *k*-point mesh. In all of the geometry optimizations, we fixed the three bottom layers of the slab in their equilibrium positions obtained for the clean surface and allowed full relaxation of the coordinates of all of the other Pt atoms and those of the adsorbates. Geometry optimizations were performed using the VASP implementations of the conjugate-gradient and quasi-Newton algorithm and stopped when the forces on all moving atoms were smaller than 0.01 eV/Å. Vibrational frequencies of CH were computed within the harmonic approximation using the finite differences method with two (one back and one forward) displacements per atomic coordinate of the adsorbate (only) of 0.015 Å. Though DFT calculations tend to overestimate frequencies compared to experimental values,[20] frequency shifts between similar adsorption configurations are typically much better reproduced.[6]

RESULTS AND DISCUSSION

Chemisorbed methylidyne on a Pt(211) surface was produced in two steps. First, we exposed the Pt(211) surface at T_s = 150 K to a molecular beam of CH_4 with incident translational energy E_t = 65 kJ/mol to dissociate methane both on step and terrace sites.[7−9] The resulting dissociation products on the step and terrace sites were then decomposed thermally by heating the surface to 250 K, resulting in a single absorption peak A at 2972 cm^{-1} as shown in Figure 1a, which we assign to methylidyne by comparison with results reported by Trenary and co-workers for Pt(111).[1] Since T_s = 250 K is below the surface temperature needed for recombinative desorption of H_2 from the steps,[21] we assign peak A to CH(ads) with co-adsorbed H atoms.

After spectrum (a) was recorded, we performed another annealing cycle for 2 min at T_s = 310 K and cooled the sample back to T_s = 150 K. This led to a decrease in the intensity of peak A and the appearance of a redshifted absorption peak B at 2962 cm^{-1}, as shown in Figure 1b. Additional 2 min annealing cycles at T_s = 330 K and then at T_s = 350 K led to the appearance of a third RAIRS peak C at 2951 cm^{-1} and a decrease in signal for peaks A and B, as shown in traces of Figure 1c,d. The observed changes in absorption intensity from

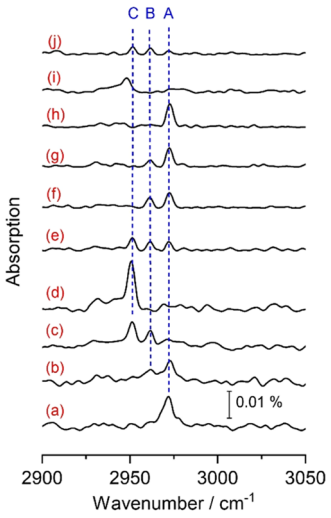

Figure 1. (a) RAIR spectrum recorded at T_s = 150 K following exposure of Pt(211) to a beam of methane with incident energy E_t = 65 kJ/mol and annealing to T_s = 250 K for 2 min. Spectra (b−d) show changes in the RAIR spectra recorded at T_s = 150 K, following 2 min annealing steps with increasing annealing temperature to reduce the H(ads) coverage: (b) T_s = 310 K, (c) T_s = 330 K, and (d) T_s = 350 K. Spectra (e−h) were observed by exposing the surface (d) to D_2 gas at T_s = 150 K with increasing D_2 dose: (e) 0.5 L, (f) 1.0 L, (g) 1.8 L, and (h) 2.3 L. Spectrum (i) recorded after renewed annealing to T_s = 350 K to remove the co-adsorbed D atoms and (j) after renewed exposure to 0.5 L of D_2 at T_s = 150 K.

peak A to C can be reversed to restore peak A by exposing the surface to increasing doses of D_2 (or H_2) gas at T_s = 150 K, leading to the spectra in Figure 1e−h. Trace (i) shows how renewed heating to T_s = 350 K reverses the intensity changes from peak A to C again and (j) shows how renewed exposure causes peaks B and A to reappear.

In conclusion, we observe reversible absorption intensity shifts between peaks A, B, and C, with changing surface hydrogen coverage except for a slow decrease in the total C−H absorption signal, which is accompanied by the appearance of three analogous C−D stretch peaks for deuterated methylidyne near 2100 cm^{-1} due to the D/H exchange (not shown).

These observations differ markedly from what was reported for methylidyne chemisorbed on Pt(111) by Trenary and co-workers,[1] who detected a single C−H stretch peak which displayed a gradual increase in vibrational frequency from 2957 to 2974 cm^{-1} with increasing hydrogen coverage.[1] The reason for this difference in the coverage-dependent frequency shift must be due to the different surface structures for the two surfaces. While on Pt(111), all surface atoms are equivalent and are arranged in a two-dimensional plane, with six equivalent nearest neighbors for each surface atom, the Pt(211) surface consists of one-dimensional rows of steps, separated by rows of terrace and corner sites labeled as (s), (t), and (c) in Figure 2a. Therefore, the observed difference for the methylidyne RAIRS spectra on Pt(111) and Pt(211) can be explained if CH(ads) adsorption takes place on the step sites of Pt(211), forming one-dimensional rows of adsorbates where each methylidyne species can have either zero, one, or two H(ads) as nearest neighbors with a probability that depends on the total hydrogen coverage.

It is worth noting that DFT calculations predict the strongest binding energy for both atomic hydrogen and methylidyne on the steps of Pt(211).[5,22,23] Whereas for H

https://doi.org/10.1021/acs.jpcc.2c07235
J. Phys. Chem. C XXXX, XXX, XXX−XXX

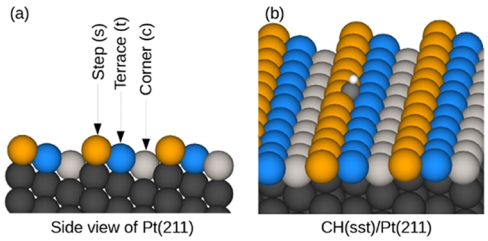

Figure 2. (a) Side view of the Pt(211) surface. Yellow, blue, and light gray spheres represent the step (s), terrace (t), and corner (c) Pt atoms, and in dark gray, we represent inner-layers Pt atoms. (b) Similar to panel (a) (in the perspective view) but with CH adsorbed on the surface in a threefold *sst* site (see text).

atoms, the preferred adsorption geometry is on the bridge sites between two step Pt atoms (referred to as ss site in what follows): methylidyne preferentially chemisorbs on a threefold site near the step: involving one t and two s Pt atoms (configuration hereafter referred to as sst, shown in Figure 2b). Therefore, the shift in relative intensity from peak A to B to C with decreasing hydrogen coverage upon surface heating can be rationalized by the changes in probability for a CH(ads) species on a step site to having either two (peak A), one (peak B), or zero (peak C) neighboring hydrogen atom.

To shed more light on this, we have made use of the ability to control the dissociation site of methane on Pt(211) by judiciously selecting the translational energy E_t of the incident methane molecules. Since the barrier for methane dissociation is lower on the step sites than on the terrace sites,[7] reducing E_t of the incident methane from 65 to 41 kJ/mol makes methane dissociation site-selective on the step sites. The left-hand side of Figure 3 shows a spectrum recorded following exposure of Pt(211) to a beam of CH_4 with E_t = 41 kJ/mol at T_s = 120 K (see trace a). At this incident energy, methane dissociation occurs only on the step sites indicated by the presence of a single absorption peak at 2904 cm^{-1} and the absence of the terrace peak, which would appear at 2889 cm^{-1}.[7] Heating the Pt(211) surface to T_s = 250 K results in the disappearance of the peak at 2904 cm^{-1} and the appearance of peak A at 2972 cm^{-1} assigned to methylidyne on the step sites with two neighboring H atoms as shown in trace b on the l.h.s. of Figure 3.

Further surface heating to T_s = 300 K caused the intensity of peak A to decrease and at T_s = 350 K to be replaced by peak C, which is assigned to CH(ads) in the step sites without co-adsorbed H(ads). Based on this observation, methyl on the step sites is confirmed to decompose into CH(ads) on the step sites.

The fate of the CH_3(ads) on terrace sites was also studied by first passivating the step sites with deuterium atoms (see the r.h.s of Figure 3). This was achieved by exposing the clean Pt(211) surface to 1 L of D_2 at T_s = 120 K. Following the passivation of the steps, an incident methane beam with E_t = 65 kJ/mol resulted in the formation of CH_3(ads) selectively on the terrace sites as indicated by a single RAIRS peak at 2889 cm^{-1} in trace (a) on the r.h.s. of Figure 3. The lack of any RAIRS signal at 2904 cm^{-1} confirms the absence of CH_3(ads) on the step sites. Following the same procedure as for the surface with CH_3(ads) on the steps, we again heated the surface to T_s = 250, 300, and 350 K (see Figure 3b–d on the right). No RAIRS signal for peaks A, B, or C was observed following the annealing steps, and the CH_3(terrace) peak vanished. This indicates that the methyl species on the terrace sites did not decompose to form methylidyne but were removed by recombinative desorption as CH_4 upon surface heating. We note that the absorption signal at saturation coverage of CH_3(ads) on terraces (Figure 3a, r.h.s) is higher than for CH_3(ads) on the step sites (Figure 3a, l.h.s), most likely due to the tilted geometry of the methyl species adsorbed on the step sites.

Further evidence is presented in Figure 4 to show that the chemisorbed methylidyne originates solely from the methyl on the steps. Figure 4 shows the RAIR spectra recorded during exposure of the Pt(211) surface at T_s = 220 K to a methane beam with translational energy of E_t = 41 kJ/mol (left) or E_t =

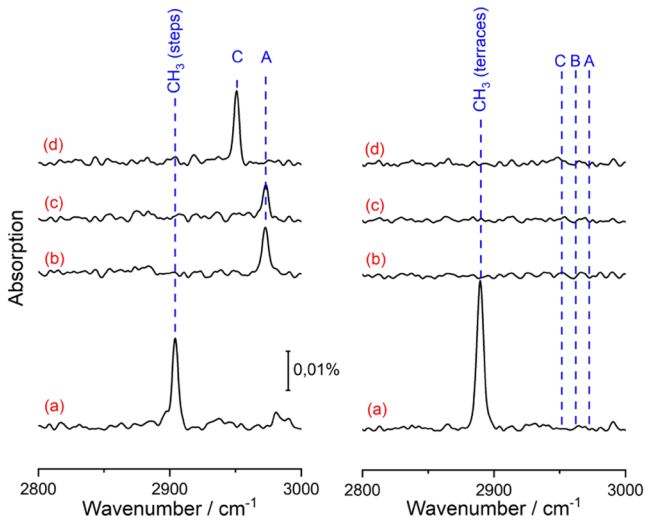

Figure 3. (a) RAIR spectra recorded following methane dissociation at T_s = 120 K with E_t = 41 kJ/mol (left) and E_t = 65 kJ/mol and passivation of the steps with deuterium (right). For traces (b–d), the surface was annealed for 2 min at increasing temperature: (b) T_s = 250 K, (c) 300 K, and (d) 350 K. Each RAIR spectrum was recorded at T_s = 120 K and is an average of 1024 scans.

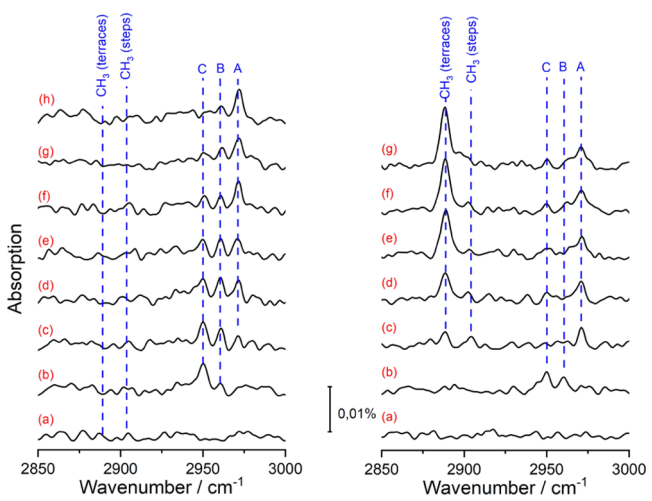

Figure 4. RAIR spectra recorded for increasing doses of methane at T_s = 220 K: (a) 0 ML, (b) 20 ML, (c) 60 ML, (d) 100 ML, (e) 140 ML, (f) 180 ML, (g) 220 ML and (h) 380 ML. The spectra on the l.h.s were obtained for a methane beam with E_t = 41 kJ/mol and those on the r.h.s for a methane beam with E_t = 65 kJ/mol. Each RAIR spectrum was recorded at T_s = 220 K and averaged over 512 scans.

https://doi.org/10.1021/acs.jpcc.2c07235
J. Phys. Chem. C XXXX, XXX, XXX−XXX

65 kJ/mol (right). With E_t = 41 kJ/mol, the methane molecules dissociate only on the step sites.[7] However, at T_s = 220 K, we do not observe the RAIRS peak at 2904 cm^{-1} corresponding to CH_3 (steps). Instead, for a dose of 20 ML CH_4 (trace b), we observe directly the formation of CH(ads) indicated by the two peaks C and B at 2951 and 2962 cm^{-1}, respectively. With increasing incident CH_4 dose, the RAIRS signal intensity shifts from peak C to B to A at 2972 cm^{-1}, indicating that at T_s = 220 K, the nascent CH_3(ads) on the steps are unstable and rapidly convert into CH(ads) and H(ads).

The r.h.s. of Figure 4 shows RAIR spectra recorded after colliding Pt(221) with CH_4 of E_t = 65 kJ/mol at T_s = 220 K. At this higher incident energy, methane dissociation occurs both on the step and the terrace sites. The strong RAIRS signal at 2889 cm^{-1} indicates that CH_3(ads) on the terrace sites is stable at T_s = 220 K, while the weak signal at 2904 cm^{-1} and the successive appearance of peaks C, B, and A show that CH_3(ads) on the step sites starts to dehydrogenate to form CH(ads) and H(ads). With increasing methane dose, we observe a shift in absorption intensity from peak C to B to A. For low methane doses, H(ads) can still diffuse along the step sites away from CH(ads), leading to the appearance of peak C first.

To confirm our assignment of RAIRS peaks A, B, and C, we performed DFT calculations for methylidyne adsorbed on Pt(211) for different hydrogen coverages. We have considered a 1 × 5 surface unit cell with one methylidyne and n co-adsorbed H atoms (n = 0, 1, 2, 3, 4). The 1 × 5 unit cell was chosen because it is the minimum size allowing calculations with up to 2 H atoms co-adsorbed in the step, where either both, only one, or none are NN of CH adsorbed in an sst site. In all calculations, CH and H were adsorbed in sst and ss sites, respectively. Since adsorption of both H and CH bound to the same two s Pt atoms is energetically highly unfavored, there are only four possible ss sites for the co-adsorbed H atoms within the 1 × 5 unit cell. In Figure 5, we show all of the explored configurations of CH with 0, 1, 2, 3, and 4 co-adsorbed H atoms in the step. They are grouped according to the number of H atoms that are nearest neighbor (NN) to CH: 0 H NN (red box), 1 H NN (green box), and 2 H NN (blue box). In Figure 5 (on the right), we also report the CH stretch frequency (in cm^{-1}) for all of the explored configurations. Again, we have used red, green, and blue to indicate the CH stretch frequencies obtained for configurations with 0 H NN, 1 H NN, and 2 H NN, respectively. Interestingly, all of the frequencies of CH obtained for configurations with the same number of H NN atoms are very close to each other, and the average frequency of each group is blueshifted with respect to those with a smaller number of H NN atoms. For instance, the average frequency for structures characterized by 1 H NN to CH (represented in green) is ~3036 cm^{-1}, which is 9 cm^{-1} larger than the average frequency of structures with 0 H NN and 5 cm^{-1} smaller than for those with 2 H NN to CH(ads). Therefore, the frequency shift between structures with the minimum and maximum possible number of H(ss) atoms NN to CH (0 and 2, respectively) is 14 cm^{-1}, which is smaller but still similar to the experimental value of 21 cm^{-1}. Actually, to reduce anharmonic effects not accounted for in our calculations, it is convenient to compare with RAIRS frequencies measured for deuterated methylidyne, CD(ads) (refer to Figure S1 in the Supporting Information). For CD(ads), the three RAIRS frequencies are 2201, 2210, and

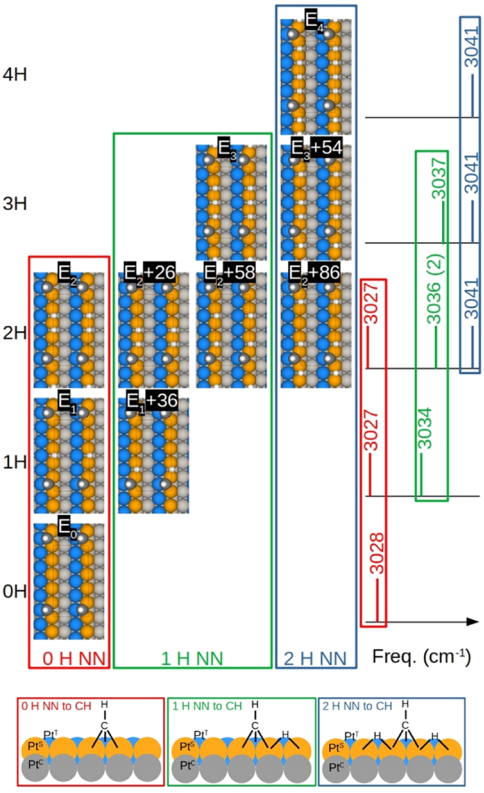

Figure 5. (CH(*sst*) + nH(ss))/Pt(211) structures (n = 0, 1, 2, 3, 4) obtained in DFT calculations. Configurations in the same row are characterized by the same value of n. E_n (n = 0, 1, 2, 3, 4) represents the energy of the most stable configuration with n co-adsorbed H atoms, and E_n + X indicates that the corresponding structure has an energy equal to E_n + X meV. On the right: CH stretch frequencies for the configurations in the same row (the number 2 in parentheses next to 3036 indicates that the two configurations with n = 2 and only 1 H NN to CH have the same frequency: 3036 cm^{-1}). Red, green, and blue boxes are used to indicate configurations and frequencies obtained with 0, 1, and 2 H(ss) atoms NN to CH(*sst*), respectively. Bottom panels: schematic representation of configurations with 0 (red box), 1 (green box), and 2 (blue box) H(ss) NN to CH(*sst*).

2217 cm^{-1}; i.e., the difference between the maximum and minimum RAIRS frequencies is 16 cm^{-1}, whereas the theoretical frequency difference is 11 cm^{-1} (the minimum and maximum theoretical frequencies are 2226 and 2237 cm^{-1}, respectively).

Thus, our DFT results are in line with the successive blue shift observed in our experiments of the C−H stretch frequency of methylidyne upon adsorption of one or two hydrogen atoms as the nearest neighbors of the CH(ads) species. Based on the data shown in Figure 1 and the results of our DFT calculations for the vibrational frequencies, we assign peak A at 2972 cm^{-1} to CH(ads) on a step site with two NN H(ads) located on either side of CH(ads), peak B at 2960 cm^{-1} to CH(ads) on a step site with only one NN H(ads) and peak C at 2950 cm^{-1} to CH(ads) on a step site without adjacent H(ads). The fact that recombinative desorption of hydrogen atoms from Pt(211) starts above T_s = 300 K explains the gradual shift in absorption intensity from A to C, while the vibrational frequencies for each of the three peaks are independent of H(ads) coverage. Cooling the Pt(211) surface to T_s = 150 K and exposure to hydrogen gas increases the

https://doi.org/10.1021/acs.jpcc.2c07235
J. Phys. Chem. C XXXX, XXX, XXX−XXX

H(ads) coverage and reverses the shift in absorption intensity, restoring peak A in trace (d) of Figure 1.

CONCLUSIONS

In conclusion, three distinct RAIRS absorption peaks were observed at 2951, 2962, and 2972 cm^{-1} following methyl dehydrogenation on the step sites of the Pt(211) surface. The relative absorption intensity of these three RAIRS peaks can be controlled in a reversible fashion simply by changing the H-atom coverage. Combined with DFT calculations, we propose that these RAIRS peaks correspond to three different hydrogen environments adjacent to the methylidyne species with either 0, 1, or 2 H atoms as the nearest neighbors. The observed changes in the RAIR spectra demonstrate that methylidyne adsorbs in the form of one-dimensional rows on the steps of Pt(211), while on Pt(111), the adsorption occurs in a two-dimensional plane.

ASSOCIATED CONTENT

Supporting Information

The Supporting Information is available free of charge at https://pubs.acs.org/doi/10.1021/acs.jpcc.2c07235.

RAIR spectra for CD_3(ads) and CD(ads) on the steps and terraces of Pt(211) (Figure S1); DFT adsorption energy, E_{ads} for the (CH + nH) configurations on the steps of Pt(211), where n refers to the number of co-adsorbed H atoms (Figure S2) (PDF)

AUTHOR INFORMATION

Corresponding Authors

H. Fabio Busnengo − *Facultad de Ciencias Exactas, Ingeniería y Agrimensura, Universidad Nacional de Rosario, 2000 Rosario, Argentina; Grupo de Fisicoquímica en Interfaces y Nanoestructuras, Instituto de Física Rosario (IFIR), CONICET-UNR, 2000 Rosario, Argentina;* orcid.org/0000-0002-7532-8495; Email: busnengo@ifir-conicet.gov.ar

Rainer D. Beck − *Institute of Chemical Sciences and Engineering (ISIC), École Polytechnique Fédérale de Lausanne (EPFL), 1015 Lausanne, Switzerland;* orcid.org/0000-0002-8152-8290; Email: rainer.beck@epfl.ch

Authors

Harmina Vejayan − *Institute of Chemical Sciences and Engineering (ISIC), École Polytechnique Fédérale de Lausanne (EPFL), 1015 Lausanne, Switzerland*

Ana Gutiérrez-González − *Institute of Chemical Sciences and Engineering (ISIC), École Polytechnique Fédérale de Lausanne (EPFL), 1015 Lausanne, Switzerland*

María E. Torio − *Facultad de Ciencias Exactas, Ingeniería y Agrimensura, Universidad Nacional de Rosario, 2000 Rosario, Argentina; Centro Internacional Franco Argentino de Ciencias de la Información y de Sistemas (CIFASIS), CONICET-UNR, 2000 Rosario, Argentina*

Complete contact information is available at: https://pubs.acs.org/10.1021/acs.jpcc.2c07235

Notes

The authors declare no competing financial interest.

ACKNOWLEDGMENTS

This work has been supported by the Consejo Nacional de Investigaciones Científicas Técnicas (CONICET), the Ministerio de Ciencia, Tecnología e Innovación (MCTI) of Argentina, the Swiss National Science Foundation under the Argentinian−Swiss Joint Research Program (ASJRP) Project No. IZSAZ2-173328, the ANPCyT Project PICT No. 2750 (MCTI-Argentina), and UNR PID projects ING534 and 80020180100121UR. All calculations have been performed in the CCT-Rosario Computational Center, a member of the High-Performance Computing National System (SNCAD, MCTI-Argentina).

REFERENCES

(1) Deng, R.; Herceg, E.; Trenary, M. Characterization of Methylidyne on Pt(111) with Infrared Spectroscopy. *Surf. Sci.* **2004**, *573*, 310−319.

(2) Overett, M. J.; Hill, R. O.; Moss, J. R. Organometallic Chemistry and Surface Science: Mechanistic Models for the Fischer−Tropsch Synthesis. *Coord. Chem. Rev.* **2000**, *206−207*, 581−605.

(3) Zhang, H.; Sun, Z.; Hu, Y. H. Steam Reforming of Methane: Current States of Catalyst Design and Process Upgrading. *Renewable Sustainable Energy Rev.* **2021**, *149*, No. 111330.

(4) Pal, D. B.; Chand, R.; Upadhyay, S. N.; Mishra, P. K. Performance of Water Gas Shift Reaction Catalysts: A Review. *Renewable Sustainable Energy Rev.* **2018**, *93*, 549−565.

(5) Chen, Y.; Vlachos, D. G. Hydrogenation of Ethylene and Dehydrogenation and Hydrogenolysis of Ethane on Pt(111) and Pt(211): A Density Functional Theory Study. *J. Phys. Chem. C* **2010**, *114*, 4973−4982.

(6) Torio, M. E.; Busnengo, H. F. Site-Specific Product Selectivity of Stepped Pt Surfaces for Methane Dehydrogenation. *J. Phys. Chem. C* **2020**, *124*, 19649−19654.

(7) Chadwick, H.; Guo, H.; Gutiérrez-González, A.; Menzel, J. P.; Jackson, B.; Beck, R. D. Methane Dissociation on the Steps and Terraces of Pt(211) Resolved by Quantum State and Impact Site. *J. Chem. Phys.* **2018**, *148*, No. 014701.

(8) Gutiérrez-González, A.; Crim, F. F.; Beck, R. D. Bond Selective Dissociation of Methane (CH3D) on the Steps and Terraces of Pt(211). *J. Chem. Phys.* **2018**, *149*, No. 074701.

(9) Gutiérrez-González, A.; Torio, M.; Busnengo, H.; Beck, R. Site Selective Detection of Methane Dissociation on Stepped Pt Surfaces. *Top. Catal.* **2019**, *62*, 859−873.

(10) Zaera, F. New Advances in the Use of Infrared Absorption Spectroscopy for the Characterization of Heterogeneous Catalytic Reactions. *Chem. Soc. Rev.* **2014**, *43*, 7624−7663.

(11) Hayden, B. E. Reflection Absorption Infrared Spectroscopy. In *Vibrational Spectroscopy of Molecules on Surfaces*; Yates, J. T.; Madey, T. E., Eds.; Springer: US: Boston, MA, 1987; pp 267−344.

(12) Chen, L.; Ueta, H.; Bisson, R.; Beck, R. D. Quantum State-Resolved Gas/Surface Reaction Dynamics Probed by Reflection Absorption Infrared Spectroscopy. *Rev. Sci. Instrum.* **2013**, *84*, No. 053902.

(13) Blöchl, P. E. Projector Augmented-Wave Method. *Phys. Rev. B* **1994**, *50*, 17953−17979.

(14) Kresse, G.; Hafner, J. Ab Initio Molecular Dynamics for Liquid Metals. *Phys. Rev. B* **1993**, *47*, 558−561.

(15) Kresse, G.; Hafner, J. Ab Initio Molecular-Dynamics Simulation of the Liquid-Metal–Amorphous-Semiconductor Transition in Germanium. *Phys. Rev. B* **1994**, *49*, 14251−14269.

(16) Kresse, G.; Furthmüller, J. Efficiency of Ab-Initio Total Energy Calculations for Metals and Semiconductors Using a Plane-Wave Basis Set. *Comput. Mater. Sci.* **1996**, *6*, 15−50.

(17) Kresse, G.; Furthmüller, J. Efficient Iterative Schemes for Ab Initio Total-Energy Calculations Using a Plane-Wave Basis Set. *Phys. Rev. B* **1996**, *54*, 11169−11186.

(18) Kresse, G.; Joubert, D. From Ultrasoft Pseudopotentials to the Projector Augmented-Wave Method. *Phys. Rev. B* **1999**, *59*, 1758−1775.
(19) Perdew, J. P.; Burke, K.; Ernzerhof, M. Generalized Gradient Approximation Made Simple. *Phys. Rev. Lett.* **1996**, *77*, 3865−3868.
(20) Laury, M. L.; Carlson, M. J.; Wilson, A. K. Vibrational Frequency Scale Factors for Density Functional Theory and the Polarization Consistent Basis Sets. *J. Comput. Chem.* **2012**, *33*, 2380−2387.
(21) Kolb, M. J.; Garden, A. L.; Badan, C.; Torres, J. A. G.; Skúlason, E.; Juurlink, L. B. F.; Jónsson, H.; Koper, M. T. M. Elucidation of Temperature-Programmed Desorption of High-Coverage Hydrogen on Pt(211), Pt(221), Pt(533) and Pt(553) Based on Density Functional Theory Calculations. *Phys. Chem. Chem. Phys.* **2019**, *21*, 17142−17151.
(22) Ghassemi, E. N.; Smeets, E. W. F.; Somers, M. F.; Kroes, G.-J.; Groot, I. M. N.; Juurlink, L. B. F.; Füchsel, G. Transferability of the Specific Reaction Parameter Density Functional for H2 + Pt(111) to H2 + Pt(211). *J. Phys. Chem. C* **2019**, *123*, 2973−2986.
(23) Olsen, R. A.; Bădescu, Ş. C.; Ying, S. C.; Baerends, E. J. Adsorption and Diffusion on a Stepped Surface: Atomic Hydrogen on Pt(211). *J. Chem. Phys.* **2004**, *120*, 11852−11863.

https://doi.org/10.1021/acs.jpcc.2c07235
J. Phys. Chem. C XXXX, XXX, XXX−XXX